

# Biomimetic mineralization using matrix vesicle nanofragments

Yosuke Kunitomi,<sup>1,2†</sup> Emilio Satoshi Hara,<sup>1†</sup> Masahiro Okada,<sup>1</sup> Noriyuki Nagaoka,<sup>3</sup> Takuo Kuboki,<sup>4</sup> Takayoshi Nakano,<sup>5</sup> Hiroshi Kamioka,<sup>2</sup> Takuya Matsumoto<sup>1</sup>

<sup>1</sup>Department of Biomaterials, Okayama University Graduate School of Medicine, Dentistry and Pharmaceutical Sciences, Okayama, Japan

<sup>2</sup>Department of Orthodontics, Okayama University Graduate School of Medicine, Dentistry and Pharmaceutical Sciences, Okayama, Japan

<sup>3</sup>Advanced Research Center for Oral and Craniofacial Sciences, Okayama University Graduate School of Medicine, Dentistry and Pharmaceutical Sciences, Okayama, Japan

<sup>4</sup>Department of Oral Rehabilitation and Regenerative Medicine, Okayama University Graduate School of Medicine, Dentistry and Pharmaceutical Sciences, Okayama, Japan

<sup>5</sup>Division of Materials and Manufacturing Science, Graduate School of Engineering, Osaka University, Osaka, Japan

Received 2 August 2018; revised 2 November 2018; accepted 26 November 2018

Published online 11 February 2019 in Wiley Online Library (wileyonlinelibrary.com). DOI: 10.1002/jbm.a.36618

**Abstract:** *In vitro* synthesis of bone tissue has been paid attention in recent years; however, current methods to fabricate bone tissue are still ineffective due to some remaining gaps in the understanding of real *in vivo* bone formation process, and application of the knowledge in bone synthesis. Therefore, the objectives of this study were first, to perform a systematic and ultrastructural investigation of the initial mineral formation during intramembranous ossification of mouse calvaria from a material scientists' viewpoint, and to develop novel mineralization methods based on the *in vivo* findings. First, the very initial mineral deposition was found to occur at embryonic day E14.0 in mouse calvaria. Analysis of the initial bone formation process showed that it involved the following distinct steps: collagen

secretion, matrix vesicle (MV) release, MV mineralization, MV rupture, and collagen fiber mineralization. Next, we performed *in vitro* mineralization experiments using MVs and hydrogel scaffolds. Intact MVs embedded in collagen gel did not mineralize, whereas, interestingly, MV nanofragments obtained by ultrasonication could promote rapid mineralization. These results indicate that mechanically ruptured MV membrane can be a promising material for *in vitro* bone tissue synthesis. © 2019 The Authors. *Journal Of Biomedical Materials Research Part A* Published By Wiley Periodicals, Inc. J Biomed Mater Res Part A: 107A: 1021–1030, 2019.

**Key Words:** bioinspired mineralization, matrix vesicle nanofragments, hydrogel, apatite, bone

---

**How to cite this article:** Kunitomi Y, Hara ES, Okada M, Nagaoka N, Kuboki T, Nakano T, Kamioka H, Matsumoto T. 2019. Biomimetic mineralization using matrix vesicle nanofragments. *J Biomed Mater Res Part A* 2019;107A:1021–1030.

---

## INTRODUCTION

Biomimetic mineralization involves complex spatio-temporal sequences of chemical reactions, controlled in part by the cells. Despite the large number of reports in this field and the well-documented literature, there still remain some gaps between the mechanism of mineral formation and its application in *in vitro* bone tissue synthesis. For instance, three dimensional bone tissue development has been achieved with osteoblastic cell lines, or osteoblast differentiation of stem cells; however, it is still time-consuming, requiring approximately 21 days.<sup>1,2</sup> Optimization of these techniques for synthetic bone tissue fabrication could allow the development of novel techniques to manipulate mineral formation *in vitro* for rapid synthesis of bone tissue *in vitro*, as well as novel materials for

biomedical application. Therefore, a multidisciplinary approach is necessary for understanding real tissue development and for engineering applications in mimicking the *in vivo* process.

Bone is formed through two different modes: chondrocyte-based endochondral ossification and osteoblast-based intramembranous ossification.<sup>3–6</sup> In endochondral ossification, a recent article demonstrated that chondrocyte membrane nanofragments are nucleation site for mineral formation, and artificial cell membrane nanofragments can be used as material for *in vitro* mineralization.<sup>3</sup> On the other hand, in intramembranous ossification, a major concept addresses that osteoblasts secrete matrix vesicles (MVs), which are enriched in pyrophosphatase and tissue non-specific alkaline phosphatase (TNAP). Upon calcium influx into MVs, which is

Additional Supporting Information may be found in the online version of this article.

†These authors contributed equally to this work.

**Correspondence to:** Takuya Matsumoto; e-mail: tmatsu@md.okayama-u.ac.jp

Contract grant sponsor: JSPS KAKENHI; contract grant number: JP18H05254 and JP25220912 and JP16H05533 and JP16H06990 and JP18K17119

This is an open access article under the terms of the Creative Commons Attribution-NonCommercial-NoDerivs License, which permits use and distribution in any medium, provided the original work is properly cited, the use is non-commercial and no modifications or adaptations are made.

hypothesized to be through the ability of annexin-V to bind to calcium, initial crystal deposition occurs inside the MVs.<sup>4-6</sup> Subsequently, the crystals grow, rupture the MV membrane and expand beyond the MVs limit throughout the extracellular matrix (ECM).<sup>4-7</sup> Based on this knowledge, previous attempt to induce bone formation using MVs were unable to indicate the critical role of MVs as nucleation factor.<sup>8</sup> Bone formation using cells, on the other hand, is known to require extended period of time (2-4 weeks).<sup>1,9</sup> Therefore, additional modifications in bone synthesis methods are still required.

In this study, first, in order to obtain a detailed information of the events during the initial steps of *in vivo* bone formation, we performed a systematic search and identification of the initial minerals formed during mouse calvaria development. The data showed that the initial stages of calvaria mineralization involves fibrous collagen network formation followed by MV secretion by osteoblasts. Next, MVs were isolated from MC3T3-E1 osteoblasts and embedded in hydrogel for fabrication of mineralized tissue *in vitro*. Although intact MVs show poor mineralization ability, the ruptured MV nano-fragments could promote fast mineralization within 7 days.

## MATERIAL AND METHODS

### Animals and calvaria sample isolation and preparation

Pregnant ICR mice ( $n = 30$ ) were purchased from Japan SCL Inc. (Hamamatsu, Japan), or Charles River Laboratories JAPAN (Kanagawa, Japan). All animals were handled according to the Guidelines for Animal Research of Okayama University, under the approval of the Animal Care and Use Committee of Okayama University (OKU-2015539 and OKU-2016184).

Pregnant mice from 13.5 to 15.5 days post-coitum were euthanized after overdose inhalation of isoflurane (Pfizer, New York, NY, USA). Embryos were isolated from the pregnant mice, and kept in sterilized phosphate buffer solution (PBS) on ice. Calvaria samples were then harvested from the embryos at embryonic day 13.5 (E13.5) to E15.5 and fixed with 4% paraformaldehyde (PFA, Sigma-Aldrich, St. Louis, MO, USA) for at least 20 min. For detection of the mineralized area, fixed samples were stained with Alizarin red S (Sigma-Aldrich) solution (1%) for 3 min, as reported previously.<sup>10</sup> Samples were then washed thoroughly to remove excess of staining solution and were observed under a microscope (Biozero BZ-X700, Keyence, Osaka, Japan). Calcified area was quantified using ImageJ software (NIH, Bethesda, MD, USA) by determining the total area of the delineated (calcified) area.

For identification of the very initially formed minerals with calcein, pregnant mice were injected calcein (20 mg/kg) 1 day before euthanasia. Immediately after euthanasia, embryos were isolated from the pregnant mice and observed under a fluorescent stereoscopic microscope (SZX12, Olympus, Tokyo, Japan). For comparison of the vascular network and mineral formation shape, E14.0 embryos were collected from calcein-injected pregnant mice, euthanized, and then intravenously injected with isolectin GS-IB4 conjugated with Alexa Fluor-594 (Life Technologies, Carlsbad, CA, USA) using an ultra-thin 34G (200  $\mu\text{m}$ ) needle, for detection of blood vessel distribution in calvaria.

For analysis of the morphology change of crystals during tissue maturation, calvaria samples were harvested from E14.5 to E15.5 embryos, as well as from post-natal day 7 (P7) newborn mice ( $n = 3$ ) and 6-week-old adult mice ( $n = 3$ ).

### X-ray micro computed tomography (micro-CT)

Micro-CT images of the collected calvaria samples were obtained using a SkyScan 1174 compact micro-CT (SkyScan, Aartselaar, Belgium). CT scans were performed at a resolution of 6.5  $\mu\text{m}$ , and scanned sections were reconstructed for formation of the final 3D images using Nrecon and CTVol SkyScan softwares. Bone volume was analyzed under the same parameters, using CTAn SkyScan software.

### Field emission scanning electron microscopy (FE-SEM) and transmission electron microscopy (TEM)

For FE-SEM observation, samples were fixed and prepared based on the protocol described previously.<sup>3</sup> In brief, femur epiphysis samples were collected, fixed in 2% glutaraldehyde/2% PFA solution for 24 h, washed with phosphate buffered saline (PBS), processed with a solution containing 3% potassium ferrocyanide (Sigma-Aldrich) in PBS with an equal volume of 4% w/v aqueous solution of osmium tetroxide (TAAB Laboratories Equipment Ltd., Berkshire, UK). The tissues were incubated in this solution for 1 h on ice. Samples were then washed thoroughly and incubated with freshly prepared 1% thiocarbonylhydrazide (Sigma-Aldrich) solution for 20 min at room temperature. Tissues were washed thoroughly and incubated with 1% osmium for 30 min at room temperature. After wash, samples were dehydrated to a sequence of ethanol and acetone, and finally embedded in EPON 812 resin (TAAB Laboratories Equipment Ltd.). Specimens were then polished and cross-sectioned by an argon ion etching (SM-090101 Cross Section Polisher; JEOL, Tokyo, Japan). Specimens were then observed by FE-SEM (JSM-6701F, JEOL) with backscattered electron, operated at 5 kV using an annular semi-conductor detector.

Resin-embedded calvaria samples, previously observed by FE-SEM, were then sliced in 80 nm thick slices with diamond knife for observation in a transmission electron microscope (TEM; JEM-2100, JEOL), according to methods described previously.<sup>3</sup> TEM observation of calcospherites was followed by electron diffraction.

For analysis of mineral cluster morphology, isolated embryonic calvaria were immediately immersed in NaOCl solution for approximately 10 min for dissolution of organic matter. Next, the remaining minerals were washed thoroughly with distilled water and subsequently dehydrated with 100% ethanol. Next, the samples were allowed to dry at room temperature, and were then placed onto an aluminum holder, and submitted to osmium coating (Neoc-STB, Meiwaofosis, Tokyo, Japan) before FE-SEM observation.

### Image analysis

Image analyses were performed with ImageJ software (NIH, Bethesda, MD, USA). For quantitative analysis of the alizarin red stained area, the total mineralized area was

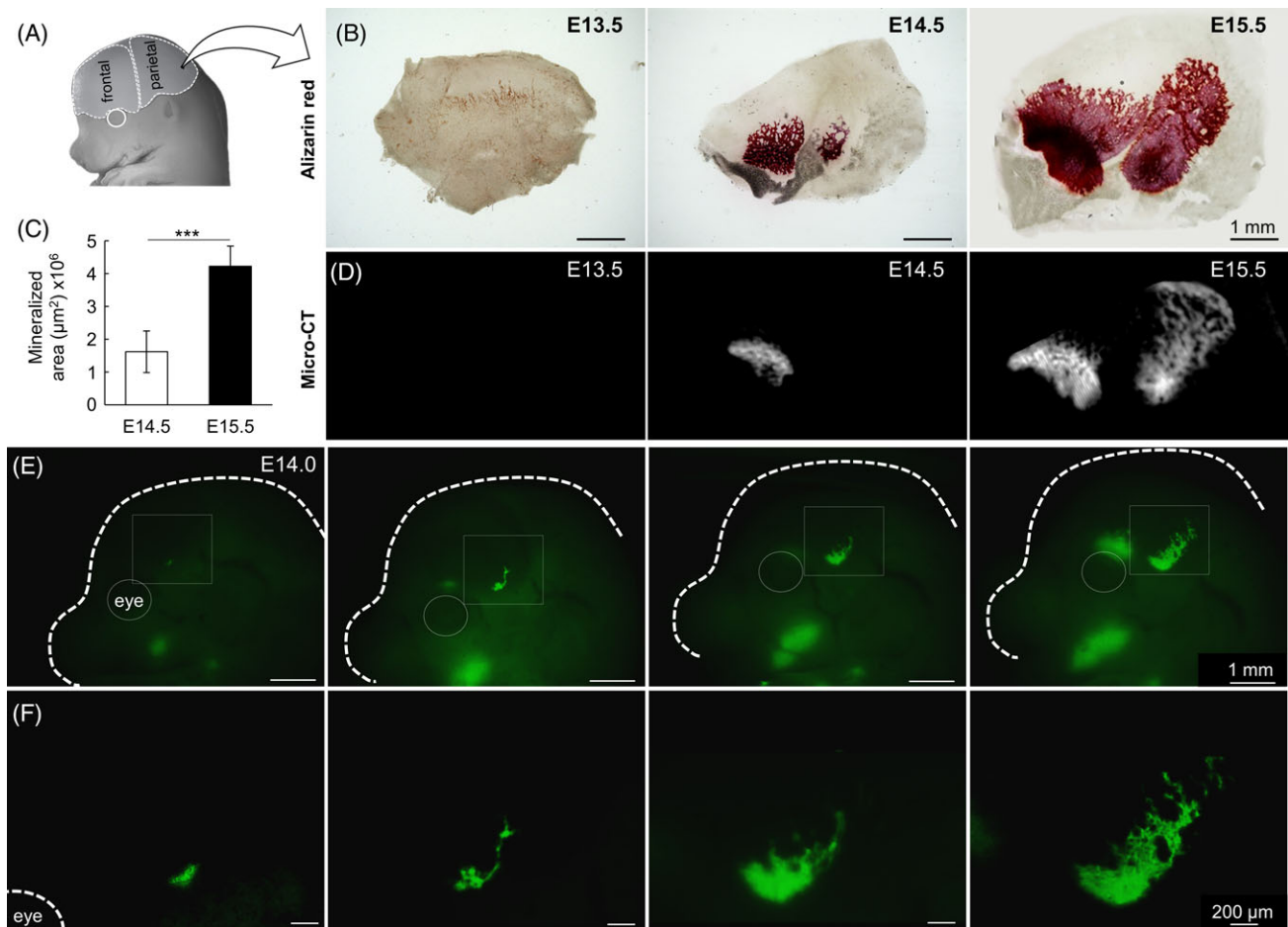


**FIGURE 1.** (A) Photograph of an embryo head, showing the area of the tissue isolated for all experiments. Bone formation was analyzed in both frontal and parietal bones. (B) Panoramic view of alizarin red S staining of mouse calvaria, showing initial mineralization at E14.5. (C) Quantitative analysis of the mineralized area in frontal and parietal bones of E14.5 and E15.5 calvaria. \*\*\* $p < 0.001$ , Students'  $t$ -test. (D) Three-dimensional reconstruction of microCT scanned (6.5  $\mu\text{m}$  resolution) calvaria from E13.5 to E15.5 confirming initial mineralization at E14.5. Images are representative of three different samples. (E,F) Photographs of initial minerals labeled with calcein in different embryos at E14.0. Note the growth pattern of the minerals. Lower panels (F) are high magnification images of the areas inside the squares in E.

first delineated, and the surface area was determined. Average was taken from three different calvaria samples.

The length of mineralized tissue in alizarin red stained samples was measured by obtaining the average value of the linear distance from a spot in the center region axially toward the foremost ends, determined randomly. Average was taken from at least 16 linear distances. The measurements were based on three different calvaria bones stained with alizarin red (total of 50 measurements).

The thickness of minerals in E14.5 and E15.5 was performed by determining the thickness of initial bone layers in SEM images of resin-embedded calvaria. Quantitative analysis was based on the average and standard deviation of >100 measurements, in total. Each measurement was performed at three independent sites (17 measurements per site), selected randomly, from two different samples at each embryonic stage (E14.5 and E15.5).

The surface area of each MV or calcospherite was determined after delineation of the MV or calcospherite boundaries. Quantitative analysis was based on the average and standard deviation of at least 30 MVs or 50 calcospherites.

### Fluorescence staining and immunohistochemical analysis

Samples previously fixed with PFA, were washed in PBS, blocked with blocking solution (Blocking One Histo, Nacalai Tesque, Kyoto, Japan) and then immunolabeled with primary antibody, or the isotype-matched IgG antibody at 4°C overnight.<sup>11</sup> Primary antibodies were rabbit polyclonal anti-connexin 43, rabbit monoclonal anti-type I collagen, and rabbit polyclonal integrin  $\alpha 5$ , all from Abcam (Cambridge, UK). The target primary proteins were then visualized after incubation with secondary antibody conjugated with Alexa Fluor 488 or 647 (Life Technologies) under a multiphoton laser scanning confocal microscope (LSM780, Zeiss, Jena, Germany). Cell nuclei was stained with Hoechst-3334 (Life Technologies). Cell membrane staining was performed with FM4-64 (Life Technologies), according to the manufacturer's instructions.

### Cell culture and *in vitro* mineralization

MC3T3-E1 osteoblastic cells were maintained in Alpha Modified Eagle Medium ( $\alpha$ -MEM, Wako Pure Chemical Industries, Osaka,

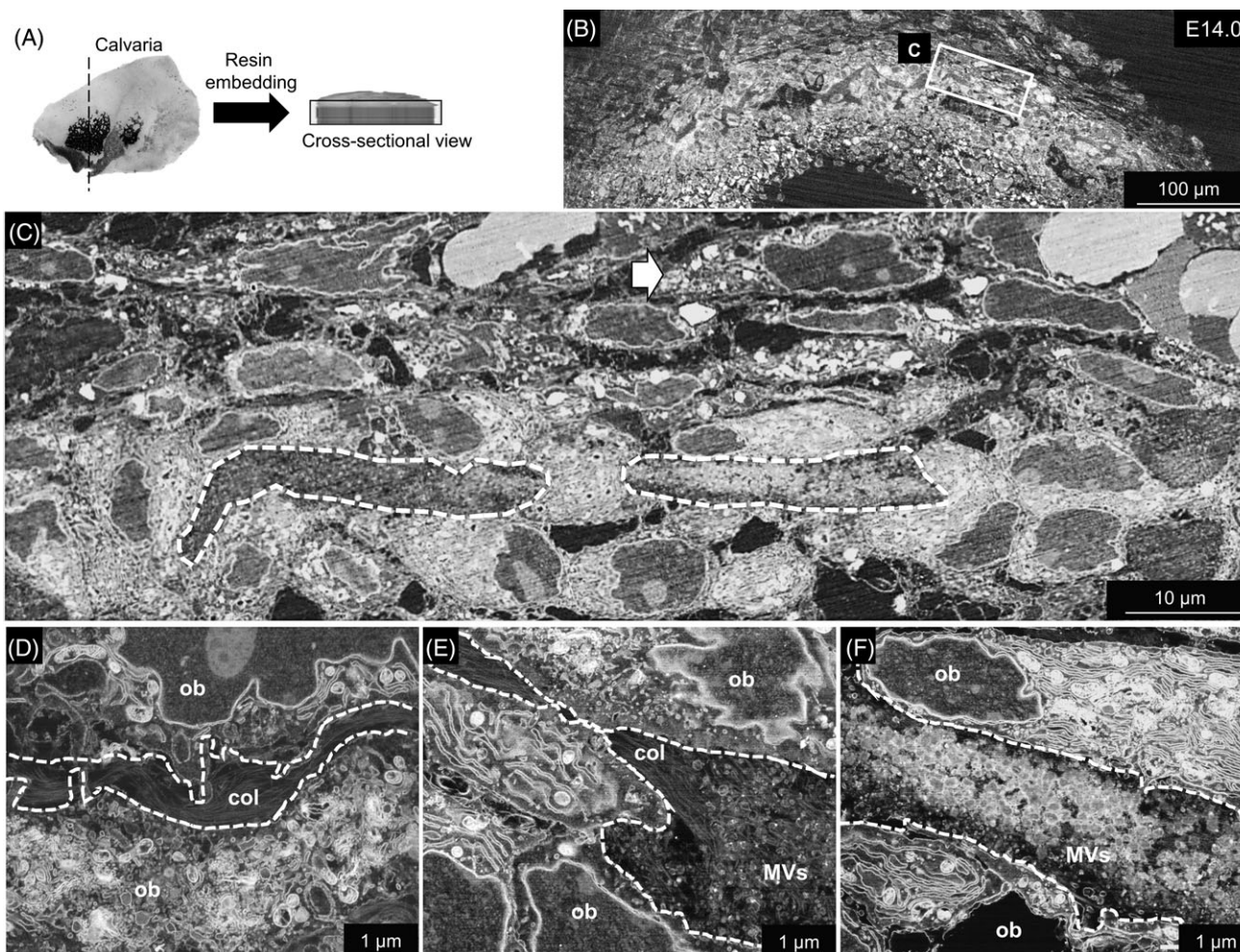


**FIGURE 2.** (A) Schematic design showing resin embedding of calvaria for cross-sectional observation. Initial minerals in E14.0 calvaria were first observed under a fluorescence stereoscope microscope, and a 2 mm<sup>2</sup> tissue was excised for further resin embedding and SEM observation. (B–F) SEM images (cross-sectional view) of E14.0 calvaria identifying the initial steps of mineral formation. (B) Low magnification image of the calvaria, in the region where initial minerals had been previously identified by calcein labeling. (C) Higher magnification of the area shown inside the square in B. Note high-contrast MVs with initial minerals in the delineated area in the right side. Note also that osteoblasts (ob) near the collagen-MV secreted area show intense ER activity, compared to those in distant areas (arrow). (D) Photograph depicting collagen secreted by osteoblasts. (E) Photograph shows MV release following the collagen secretion. (F) Photograph shows high-contrast MVs, indicating mineral formation inside the MVs. col = collagen, separated by dotted lines. ob = Osteoblasts. MVs = matrix vesicles.

Japan) containing 10% fetal bovine serum (FBS; Life Technologies) and 1% penicillin and streptomycin (Sigma-Aldrich). Cells were cultured in normal culture medium until confluency, and then cultured in osteogenic medium for 5 or 7 days. Osteogenic medium was prepared by addition of 0.1 mM L-ascorbic acid phosphate (Sigma-Aldrich), 10 mM  $\beta$ -glycerophosphate (Sigma-Aldrich) and 100  $\mu$ M dexamethasone (Sigma-Aldrich). Osteogenic medium was then harvested and submitted to centrifugation at 1000 $\times g$  for 10 min to remove dead cells and large debris, and at 150,000 $\times g$  for 60 min for isolation of MVs, based on a previously reported method.<sup>12</sup>

For *in vitro* mineralization assays, isolated MVs were directly embedded in collagen hydrogel (Cellmatrix type I-A, Nitta gelatin, Osaka, Japan) or treated mechanically with ultrasonication (Handy sonic UR-20P, Tomy Seiko Ltd, Tokyo, Japan) for 30 s before hydrogel embedding, and then

incubated in  $\alpha$ -MEM containing 10 mM  $\beta$ -glycerophosphate for 7 days for mineralization. The volume ratio of collagen/MVs was 1:1. The gelation time of collagen gel was set to 10 min. After 7 days of culture, hydrogels containing MVs were then fixed with 4% PFA for at least 1 h, and stained for mineral formation with alizarin red S.

For TEM observation of MVs, freshly isolated MVs were fixed with 2% PFA and 2% glutaraldehyde for 30 min, centrifuge-washed, fixed with 1% osmium tetroxide (TAAB Laboratories Equipment Ltd.) for 20 min and centrifuge-washed again. Samples were then dispersed onto grids before TEM observation (H-7650, Hitachi High-Technologies, Tokyo, Japan) at an acceleration voltage of 80 kV. For observation of MV nanofragments, freshly isolated MVs were sonicated for 30 s, and then submitted to the same steps of intact MV observation.

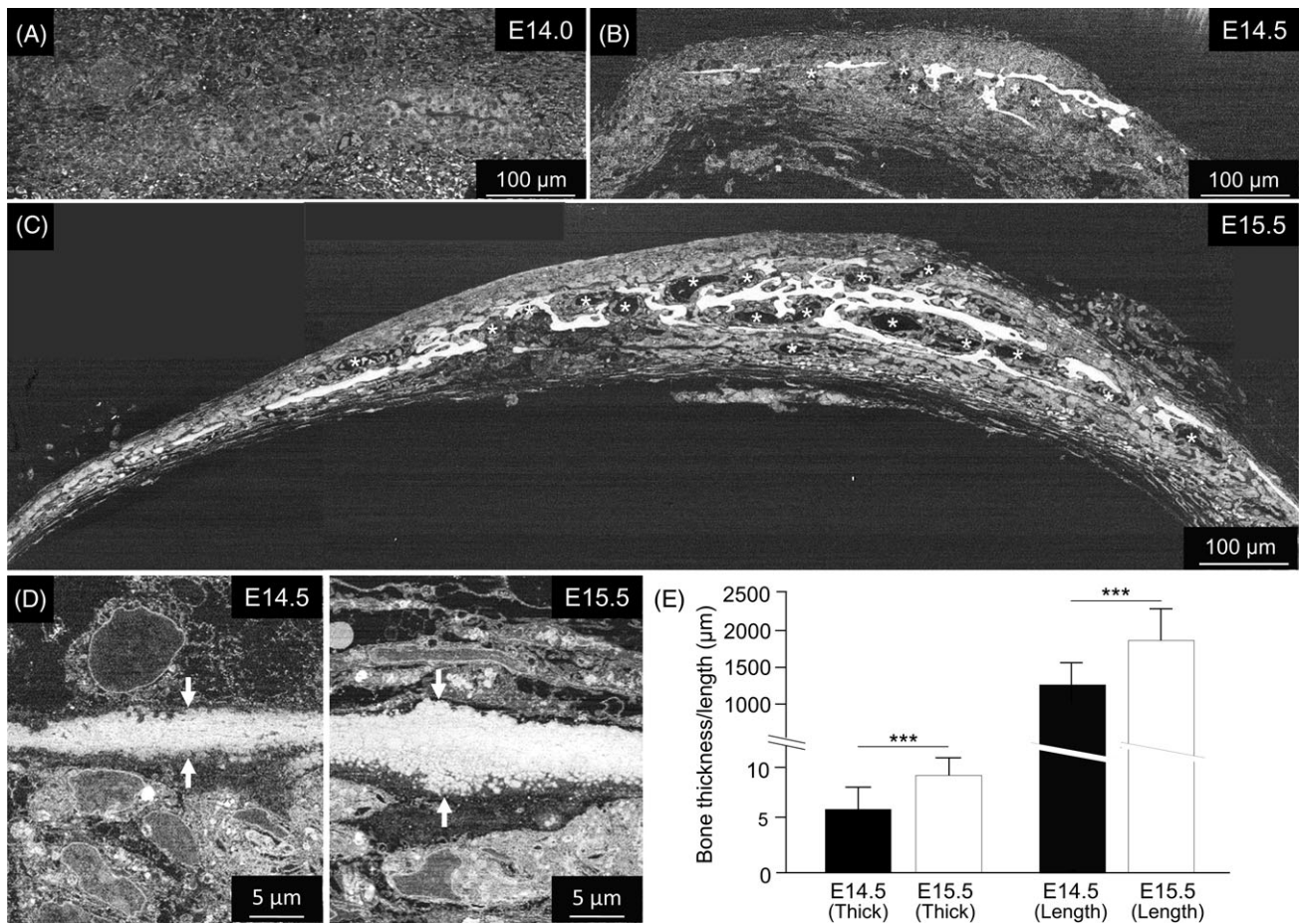


**FIGURE 3.** (A–C) SEM photographs showing mineral expansion pattern in calvaria from E14.0 to E15.5. Note that initially a single layer of minerals is formed, and subsequently bone formation expanded surrounding the blood vessels (asterisks). (D,E) SEM photographs showing how bone thickness was measured. Graph shows the average and standard deviation of >100 measurements, in total. Each measurement was performed at three independent sites (17 measurements per site), selected randomly, from two different samples, at each embryonic stage (E14.5 and E15.5). Calvarial bone length was obtained from analysis of the length of the mineralized tissue in the frontal bone only, in alizarin red stained samples. The measurements were based on three different calvaria bones stained with alizarin red (total of 50 measurements). \*\*\* $p < 0.001$ , Students'  $t$ -test.

### Statistical analysis

Analysis of the differences between groups were performed with unpaired Student's  $t$ -test, or one-way ANOVA followed by a Bonferroni post-hoc correction test when appropriate. Statview software (version 5.0; SAS Institute Inc., Cary, North Carolina, USA) was used for the analyses.

### RESULTS

To identify the initial mineral deposition, we first performed microCT analysis (6.5 µm resolution) and alizarin red staining of mouse calvaria samples at different developmental stages [Fig. 1(A–D)]. Initial mineral formation was found at E14.5 either in the parietal bone or in the frontal bone, near the eye rim [Fig. 1(B)]. Subsequently, from E14.5 to E15.5, there was a fast expansion of minerals toward the medial region [Fig. 1(C, D)]. To identify the very initial starting point, embryos at E14.0 were isolated from calcein-injected pregnant mouse, and observed under a fluorescence stereoscopic microscope. As shown in Figure 1(E,F), the initial minerals were first observed in the parietal bone, and afterwards in the frontal bone, near the eye rim.

Next, to investigate the ultrastructural changes in organic and inorganic material during mineral formation and maturation, we observed cross-sectionally the resin-embedded E14.0, E14.5, and E15.5 samples, by FE-SEM with a backscattered electron (Figs. 2 and 3). At E14.0, we could observe the very initial minerals being deposited by osteoblasts. At this stage, before initial mineral formation, osteoblasts started to secrete collagen [Fig. 2(C,D)]. Note a high activity of endoplasmic reticulum (ER) in collagen-secreting osteoblasts [Fig. 2(C), cells in the center], which is in accordance with previous reports;<sup>13</sup> whereas osteoblasts away from the mineralization site do not show high ER activity [Fig. 2(C), cells in the upper area, indicated by arrow].

Following collagen synthesis and secretion, cells started to secrete MVs, by budding as well as by exocytosis, similar to exosomes [Fig. 2(E)].<sup>5,6</sup> Eventually, initial mineral formation was observed inside the MVs [Fig. 2(F)], in accordance with numerous previous reports.<sup>5,6</sup> As collagen is synthesized, there occur a loss of cell–cell contact, as demonstrated by the expression pattern of connexin-43 in osteoblasts (Supporting information Fig. S1). Of note, there could have a difference



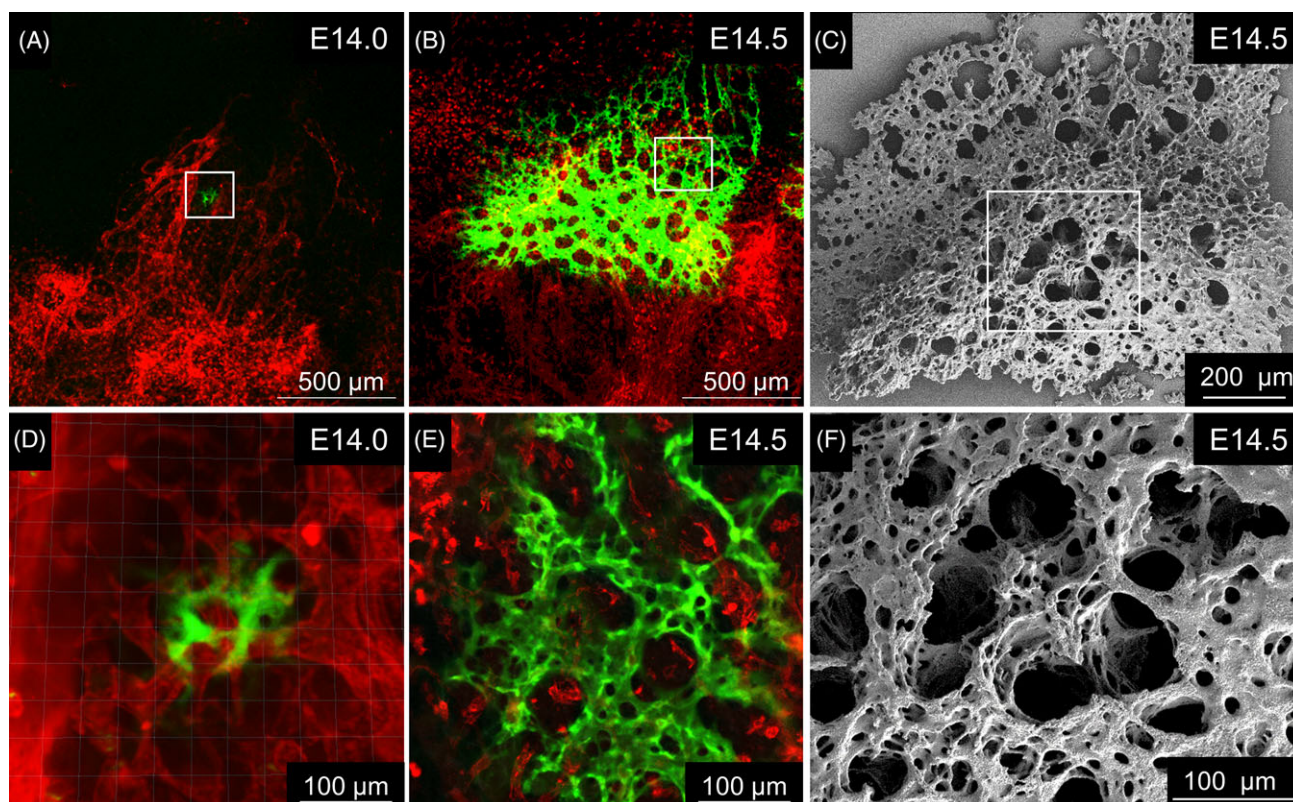


**FIGURE 4.** (A,B) Photographs of initially formed minerals near blood vessels at E14.0 and E14.5. Note that initial minerals show a mesh-like structure due to the deposition of minerals in the surroundings of blood vessels. Blood vessels were detected by isolectin (red). Minerals were labeled with calcein (green). D and E are high magnification images of the areas in the square in A and B, respectively. (C–F) SEM images of calvarial minerals after organic material dissolution with NaOCl. Note the mesh-like structure throughout the calvarial bone at E14.5. F is a high magnification image of the area inside the square in C.

between the initially synthesized collagen fibers, which are more denser and show no presence of MVs [Fig. 2(D,E)]. Additionally, initially synthesized collagen could be a template for secondary collagen assisting the orientation of mineralization. Additionally, osteoblasts started to align onto the initially deposited collagen and MVs, suggesting an initial cell polarization [Fig. 3(A,B)], which would eventually also contribute to the direction of mineral growth.

Further analysis of mineral growth pattern was then performed based on the cross-sectional views of the minerals from E14.0 to E15.5 (Fig. 3). Note a rapid mineral expansion within 12 h (E14.0–E14.5). Initially, only a single layer of minerals is deposited [Fig. 3(B)]; however, its thickness does not increase substantially [Fig. 3(D,E)]. Subsequently, the minerals are formed in the surroundings of the blood vessels [Fig. 3(B,C)]. Note that blood vessels first invade the non-mineralized calvarial tissue [Fig. 4(A)], and afterwards, the minerals are formed in the surroundings of the blood vessels, which contributes to the mesh-like structure of the calvarial bones in the early developmental stages [Fig. 4(B–F)].

Next, morphological analysis of bone crystals revealed that in the early stages of bone development (E14.5 and 15.5), the initial mineral clusters (calcospherites) are spherical and have the same size of MVs [Fig. 5(A–D)]. Therefore, the bone growth is dependent mainly on the intercellular space, and not on the size of the crystals. Gradually, the

minerals grow and achieve an elongated shape, as seen clearly in mature stages of 6 week-old mice [Fig. 5(B)]. Characterization of the minerals by electron diffraction analysis showed that all of them were hydroxyapatite [Fig. 4(B), left-down images].

Taken together, these results indicate that osteoblasts first secrete collagen fibers, to promote space for mineral formation, and then secrete MVs in large amounts to promote mineral formation. After initial mineralization inside the MVs, minerals grow and rupture the MVs, and subsequently expand toward the surrounding collagen fibers. The initial minerals formed inside the MVs still maintain a spherical shape [Fig. 5 (B), E14.5 and E15.5 samples], afterwards they become elongated and oriented minerals [Fig. 5(B), P7 and 6W samples] possibly due to mineral maturation onto collagen fibers.

Next, we attempted to induce *in vitro* mineralization using MVs and collagen hydrogel. MC3T3-E1 osteoblasts were cultured in osteogenic medium for 3–7 days, and then MVs were obtained from the culture media after ultracentrifugation [Fig. 6(A)], according to previous reported protocol.<sup>12</sup> Collected MVs were then incubated in  $\alpha$ -MEM supplemented with 10 mM  $\beta$ -glycerophosphate for another 7 days for analysis of their mineral formation ability. As shown in Figure 6(B,C), intact MVs did not promote mineral formation, which is in accordance with previous reports.<sup>8</sup> Interestingly, however, MVs nanofragments could induce

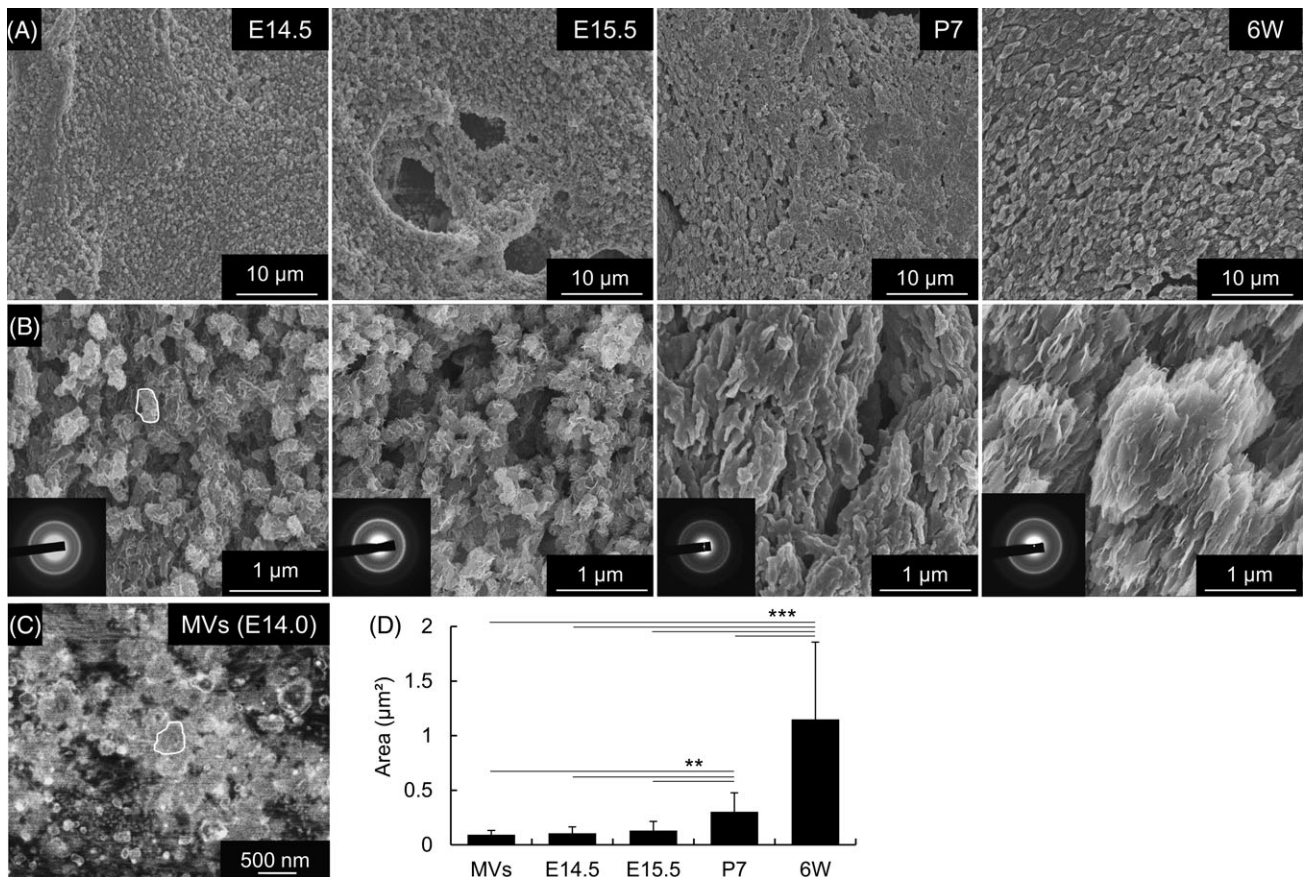


**FIGURE 5.** (A,B) SEM photographs of apatite crystals in calvaria tissues from mice at E14.5, E15.5, post-natal day 7 (P7), and 6 weeks of age. Note the growth of crystals until complete tissue maturation. (C) SEM observation with backscattered electrons of MVs. (D) Quantitative analysis (area) of MVs, and apatite crystal clusters at different developmental stages. Note that initial mineral clusters (calcospherites) present the same size of MVs (shown in C and D). Graph shows the average and standard deviation of at least 30 MVs or 50 calcospherites. Electron diffraction analysis of the minerals indicated that all of them were hydroxyapatite. \*\* $p < 0.01$ , \*\*\* $p < 0.001$ , ANOVA, Bonferroni post-hoc test.

rapid mineralization within 7 days [Fig. 6(D–G)]. Elemental analysis of the minerals by EDS, followed by electron diffraction [Fig. 6(F–H)] indicated that the *in vitro* formed minerals were hydroxyapatite.

## DISCUSSION

In this study, we identified the initial steps of mineral formation in mouse calvaria, and found that osteoblasts first release collagen fibers, which is in accordance with previous studies showing the three dimensional morphometry of collagen fibrils during initial stages of mineralization.<sup>14,15</sup> Subsequently, osteoblasts secrete MVs in large amounts and can build a large bone area of 1200  $\mu\text{m}$  in length in the initial 24 h.

Important studies on biomineralization have been carried out throughout the last decades. For instance, Irving reported important findings in the identification of phospholipids, which are the major components of plasma membranes, in the stages preceding mineralization of bones (intramembranous and endochondral ossifications) and tooth.<sup>16</sup> These phospholipids were further identified to be cell-secreted MVs<sup>5,6,17</sup>, or cell membrane nanofragments.<sup>3</sup> In the case of cell membrane nanofragments, which do not

show a spherical shape, phosphate groups in the phospholipids constituting the membranes can directly interact with calcium ions present in the extracellular environment, promoting initial mineralization. On the other hand, mineralization in MVs is known to occur at the inner side of the MV membrane. However, the mechanisms of how this mineralization occurs inside the MVs are still controversial. A major hypothesis addresses that annexins would be a major calcium-binding factor inducing calcium influx into MVs, which are rich in phosphate, and promoting mineralization.<sup>5</sup> However, mice lacking annexin-V were reported to show no significant skeletal phenotype, and the *in vitro* calcification properties of chondrocytes isolated from annexin-V knockout mouse showed no significant impairment.<sup>18–20</sup>

Additionally, phospholipids, for example, phosphatidylcholine (PC), phosphatidylserine (PS), are the major type of phospholipid in the membrane of cells. In particular, PS has been reported to have high affinity to calcium, which could then be nucleation site for mineralization.<sup>21,22</sup> However, the reason why PS does not induce mineral formation in live cells may probably involve complex inhibition process that are still unknown. Another possible explanation could be associated with the fact that PS is structurally facing the

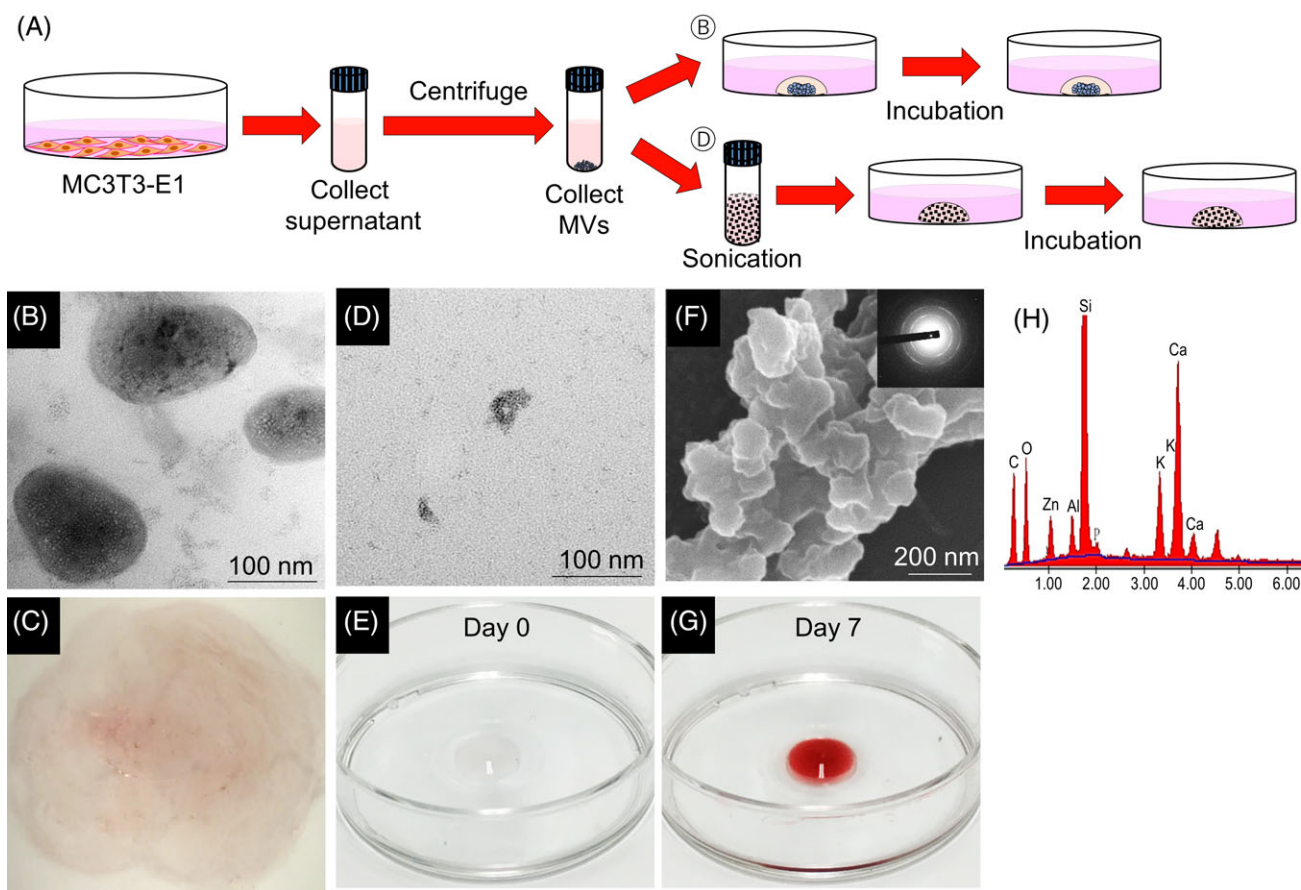


**FIGURE 6.** (A) Protocol for isolation of MVs, nanofragmentation (sonication), and mineralization *in vitro*. (B) and (D) indicate the mineralization protocol with intact MVs and MV nanofragments, respectively. (B) TEM images of isolated intact MVs. (C) Alizarin red staining of MVs cultured in collagen gel for 7 days in  $\alpha$ -MEM containing  $\beta$ -glycerophosphate. Note that intact MVs show poor mineralization ability. (D) TEM images of MV nanofragments. (E, G) Alizarin red staining of MV nanofragments embedded in collagen gel before and after mineralization. Note that, at day 0, MV nanofragments are not mineralized (no staining). Note also that MV nanofragments can mineralize within 7 days. (F) SEM image of the minerals formed inside the collagen gel containing MV nanofragments. Right upper corner: Electron diffraction analysis of the minerals showing that the minerals were hydroxyapatite. (H) EDS analysis of the minerals indicating the calcium and phosphate peaks in the minerals.

cytosolic side of the cell membrane, maintained by the enzyme flippase.<sup>23</sup> When a cell undergoes apoptosis, however, PS is catalyzed by scramblase, which allows a rapid exchange of PS between the two sides.<sup>23</sup> This PS flipping could be associated with an influx of calcium ions into the MVs and promote mineralization in the inner side.

Of note, in this article, the method for analysis of calvaria tissues was not based on a previously reported anhydrous tissue preparation.<sup>24</sup> There could have a possibility of calcium and phosphate ions to be dissolved in water-soluble solvents. However, the solubility of amorphous calcium phosphate minerals in water has been reported to be low.<sup>25</sup> Additionally, in our previous article, we have demonstrated that amorphous calcium phosphate minerals can be preserved even after preparation of thin TEM film samples, as confirmed by elemental mapping and electron diffraction.<sup>3</sup> Therefore, the results of this study indicate that an amorphous mineral phase is initially formed inside the MVs, which then crystallize into hydroxyapatite.

Following initial mineralization inside the MVs, minerals grow and rupture the MV membrane (Supporting information

Fig. S2). Consequently, the inner contents of MVs are extravasated to the surrounding nanoenvironment, facilitating mineralization of the MV-attached collagen fibers. Therefore, we hypothesized that promoting MV membrane rupture could enhance mineral formation. Indeed, when we attempted to induce mineral formation *in vitro* using MVs collected from MC3T3-E1 cells previously cultured under osteogenic medium for 5 or 7 days to enhance MVs secretion. MVs collected at day 7 already showed mineralization; therefore, we used MVs from 5-day culture. Of note, intact MVs showed poor mineralization ability. Interestingly, however, mechanical rupture of MVs allowed a rapid and direct interaction of molecules, which were confined inside the MVs, with extravascular microenvironment. A possible mechanism could be associated with early phosphatase activity (data not shown), which is known to be fundamental for bone mineralization.<sup>26</sup> Collectively, these data is in accordance with a previous article showing that nanofragments from cell membrane can also be nucleation site for mineral formation.<sup>3</sup> Therefore, nanofragmentation of cell and MV structures can be an important tool for enhancing mineralization toward *in vitro* bone tissue



synthesis. Nonetheless, isolation and collection of MVs in large amounts, which currently involves *in vitro* expansion of an enormous quantity of cells, is still a major problem hindering further development of bone tissue engineering techniques. Further understanding of the molecular mechanisms that initiate and determine mineral formation in MVs may allow the development of novel cell-independent biomaterial-based technologies for *in vitro* bone tissue synthesis.

It is worth noting that blood vessels first penetrate in the area where minerals will be formed, possibly acting as a calcium ion supplier. Several factors, such *Pdgfb*, *Tgfb*, and *Fgf*,<sup>27</sup> possibly secreted by the tissue resident osteoblasts, could be involved in the mechanisms of angiogenesis in the initial stages of calvarial tissue development. Additionally, since the minerals are formed in the surroundings of the blood vessels, initial calvaria presents with a mesh-like structure. These observations are in accordance with a recent report showing that blood vessels coordinate tissue morphogenesis, and determine bone shape by forming a template of collagen type I for deposition of bone matrix.<sup>28</sup> Based on these data, future experimentations, using a combination of ruptured MVs and different cells (e.g., endothelial cells and osteoblasts) may enable further improvement in the methods for bioengineering 3D bone tissue *in vitro*.

## CONCLUSION

In this study, we identified and characterized the initially formed apatite crystals during calvaria development. Additionally, we propose a model of biomineralization by application of mechanical stimulation for MV nanofragmentation, in order to promote rapid interaction of molecules and mineralization factors which were inside the MVs. These data may facilitate the development of further approaches and new materials for bone tissue engineering *in vitro*.

## ACKNOWLEDGMENTS

This study was supported by JSPS KAKENHI Grant Number (JP18K17119, JP16H06990, JP16H05533, JP25220912, and JP18H05254).

## AUTHOR'S CONTRIBUTIONS

Y.K. and E.S.H. designed and performed the experiments, collected analyzed the data, prepared figures and wrote the manuscript. M.O. designed part of the experiments, analyzed data. N.N. performed electron microscope analysis, as well as electron diffraction analysis. T.K., T.N., and H.K. supplied materials and equipment. T.M. designed the experiments, analyzed data, wrote the manuscript and supplied materials.

## ADDITIONAL INFORMATION

The authors declare no competing financial interests.

## DATA AVAILABILITY

Data are available upon request to the corresponding author.

## CONFLICT OF INTEREST

The authors declare no competing interests.

## REFERENCES

1. Eguchi T, Watanabe K, Hara ES, Ono M, Kuboki T, Calderwood SK. Osteonin: A novel panel of MicroRNA biomarkers in osteoblastic and osteocytic differentiation from mesenchymal stem cells. *PLoS One* 2013;8:e58796.
2. Bilousova G, Jun DH, King KB, Langhe SD, Chick WS, Torchia EC, Chow KS, Klemm DJ, Roop DR, Majka SM. Osteoblasts derived from induced pluripotent stem cells form calcified structures in scaffolds both *in vitro* and *in vivo*. *Stem Cells* 2011;29:206–216.
3. Hara ES, Okada M, Nagaoka N, Hattori T, Kuboki T, Nakano T, Matsumoto T. Bioinspired mineralization using chondrocyte membrane nanofragments. *ACS Biomater Sci Eng* 2018;4:617–625.
4. Bonucci E. Biological calcification: Normal and pathological processes in the early stages. Berlin: Springer-Verlag; 2007.
5. Wuthier RE, Lipscomb GF. Matrix vesicles: Structure, composition, formation and function in calcification. *Front Biosci* 2011;17:2812–2902.
6. Anderson HC. Molecular biology of matrix vesicles. *Clin Orthop Relat Res* 1995;314:266–280.
7. Takano Y, Sakai H, Baba O, Terashima T. Differential involvement of matrix vesicles during the initial and appositional mineralization processes in bone, dentin, and Cementum. *Bone* 2000;26:333–339.
8. Boskey AL, Boyan BD, Doty SB, Feliciano A, Greer K, Weiland D, Swain LD, Schwartz Z. Studies of matrix vesicle-induced mineralization in a gelatin gel. *Bone Miner* 1992;17:257–262.
9. Hara ES, Ono M, Eguchi T, Kubota S, Pham HT, Sonoyama W, Tajima S, Takigawa M, Stuart KC, Kuboki T. MiRNA-720 controls stem cell phenotype, proliferation and differentiation of human dental pulp cells. *PLoS One* 2013;8:e83545.
10. Hara ES, Okada M, Nagaoka N, Hattori T, Iida LM, Kuboki T, Nakano T, Matsumoto T. Chondrocyte burst promotes space for mineral expansion. *Integr Biol (UK)* 2018;10:57–66.
11. Hara ES, Ono M, Pham HT, Sonoyama W, Kubota S, Takigawa M, Matsumoto T, Young MF, Olsen BR, Kuboki T. Fluocinolone acetonide is a potent synergistic factor of TGF- $\beta$ 3-associated chondrogenesis of bone marrow-derived mesenchymal stem cells for articular surface regeneration. *J Bone Miner Res* 2015;30:1585–1596.
12. Ali SY, Sajdera SW, Anderson HC. Isolation and characterization of calcifying matrix vesicles from epiphyseal cartilage. *Proc Natl Acad Sci USA* 1970;67:1513–1520.
13. Veis A. Mineralization in organic matrix frameworks. *Rev Mineral Geochem* 2003;54:249–289.
14. Hosaki-Takamiya R, Hashimoto M, Imai Y, Nishida T, Yamada N, Mori H, Tanaka T, Kawanabe N, Yamashiro T, Kamioka H. Collagen production of osteoblasts revealed by ultra-high voltage electron microscopy. *J Bone Miner Metab* 2016;34:491–499.
15. Hashimoto M, Nagaoka N, Tabata K, Tanaka T, Osumi R, Odagaki N, Hara T, Kamioka H. Three-dimensional Morphometry of collagen fibrils in membranous bone. *Integr Biol (UK)* 2017;9:868–875.
16. Irving JT. A histological stain for newly calcified tissues. *Nature* 1958;181:704–705.
17. Anderson HC. Electron microscopic studies of induced cartilage development and calcification. *J Cell Biol* 1967;35:81–101.
18. Belluoccio D, Grskovic I, Niehoff A, Schlötzer-Schrehardt U, Rosenbaum S, Etich J, Frie C, Pausch F, Moss SE, Pöschl E, Bateman JF, Brachvogel B. Deficiency of annexins A5 and A6 induces complex changes in the transcriptome of growth plate cartilage but does not inhibit the induction of mineralization. *J Bone Miner Res* 2010;25:141–153.
19. Grskovic I, Kutsch A, Frie C, Groma G, Stermann J, Schlötzer-Schrehardt U, Niehoff A, Moss SE, Rosenbaum S, Pöschl E, Chmielewski M, Rappl G, Abken H, Bateman JF, Cheah KS, Paulsson M, Brachvogel B. Depletion of annexin A5, annexin A6, and collagen X causes no gross changes in matrix vesicle-mediated mineralization, but lack of collagen X affects hematopoiesis and the Th1/Th2 response. *J Bone Miner Res* 2012;27:2399–2412.
20. Brachvogel B, Dikschas J, Moch H, Welzel H, Von Der Mark K, Hofmann C, Pöschl E. Annexin A5 is not essential for skeletal development. *Mol Cell Biol* 2003;23:2907–2913.
21. Sinn CG, Antonietti M, Dimova R. Binding of calcium to phosphatidylcholine-phosphatidylserine membranes. *Colloids Surf A Physicochem Eng Asp* 2006;282:410–419.

22. Roux M, Bloom M. Calcium binding by phosphatidylserine head-groups. Deuterium NMR study. *Biophys J* 1991;60:38–44.
23. Verhoven B. Mechanisms of phosphatidylserine exposure, a phagocyte recognition signal, on apoptotic T lymphocytes. *J Exp Med* 1995;182:1597–1601.
24. Landis WJ, Paine MC, Glimcher MJ. Electron microscopic observations of bone tissue prepared anhydrously in organic solvents. *J Ultrastruct Res* 1977;59:1–30.
25. Combes C, Rey C. Amorphous calcium phosphates: Synthesis, properties and uses in biomaterials. *Acta Biomater* 2010;6:3362–3378.
26. Millán JL. The role of phosphatases in the initiation of skeletal mineralization. *Calcif Tissue Int* 2013;93:299–306.
27. Kusumbe AP, Ramasamy SK, Adams RH. Coupling of angiogenesis and osteogenesis by a specific vessel subtype in bone. *Nature* 2014;507:323–328.
28. Ben Shoham A, CL R, Stern T, Krief S, Akiva A, Dadosh T, Sabany H, Lu Y, Kadler KE, Zelzer E. Deposition of collagen type I onto skeletal endothelium reveals a new role for blood vessels in regulating bone morphology. *Development* 2016;143:3933–3943.